KAWASAKI STEEL TECHNICAL REPORT
No.15 (October 1986)

Structural Characteristics and Application of Kawasaki Composite Slab Bridges

Keinosuke Hamada, Tomoo Kasuga, Masakatsu Sato, Sachito Tanaka

Synopsis :
Composite slab bridge has been newly developed as a simple support highway bridge. It consists of deformed flange T-shapes, bottom steel plates and expansive concrete. The depth of this bridge is much smaller than those of conventional bridges. Moreover, since steel plates act as a concrete form, erection work is very simple, rapid and safe. The structural characteristics and fatigue strength of this slab bridge has been clarified by a static bending rupture test and high-cycle fatigue test respectively. As the result of the tests, the design method has been justified and design in general is offered. Demand for this slab bridge increases every year accompanying river improvement and railway overpass projects.

The body can be viewed from the next page.

Structural Characteristics and Application of Kawasaki Composite Slab Bridges*

Keinosuke Hamada
Staff Manager,
Civil Engineering Sec.,
Engineering &
Construction Div.

Tomoo Kasuga
Civil Engineering Sec.,
Engineering &
Construction Div.

Masakatsu Sato
Dr. Engi., Senior
Researcher, Designing
Lab., Research &
Development Center,
Engineering &
Construction Div.

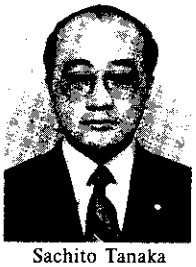

Sachito Tanaka
Designing Lab.,
Research &
Development Center,
Engineering &
Construction Div.

Synopsis:

Composite slab bridge has been newly developed as a simple support highway bridge. It consists of deformed flange T-shapes, bottom steel plates and expansive concrete. The depth of this bridge is much smaller than those of conventional bridges. Moreover, since steel plates act as a concrete form, erection work is very simple, rapid and safe. The structural characteristics and fatigue strength of this slab bridge has been clarified by a static bending rupture test and high-cycle fatigue test respectively. As the result of the tests, the design method has been justified and design in general is offered. Demand for this slab bridge increases every year accompanying river improvement and railway overpass projects.

1 Introduction

In the construction or replacement of bridges as part of river improvement projects, or in the building of railway overbridges, bridge depth is limited by a given estimated high-water level or rolling-stock gauge. On the other hand, bridge surface level is also limited by the depth of the old bridge or the elevation of access road. Particularly, in large cities like Tokyo and Osaka and their environs, land acquisition for access roads has become difficult owing to sharp rises in land prices. Therefore, the development of a new type bridge which has a lower girder depth has been strongly desired.

To meet such needs, Kawasaki Steel has developed a composite slab bridge made by filling around deformed flanges (formed by cutting deformed flange H-shapes[1] in half) with expansive concrete, as shown in **Fig. 1**. Advantages of this new bridge—such as protrusions on

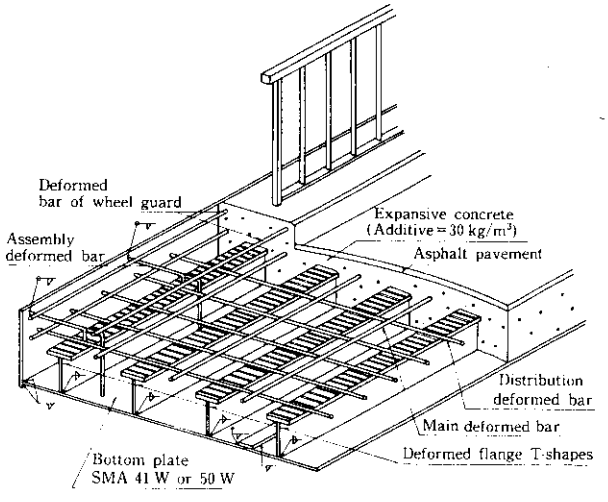

Fig. 1 Schema of composite slab bridge using deformed flange T-shapes

* Originally published in *Kawasaki Steel Giho*, **18**(1986)1,

the T-shapes functioning as a shear connector, thus permitting the use of thinner concrete covering and the use of the bottom plate as a permanent form at the time of concrete placing, thereby simplifying the execution of work and shortening the construction period—have been recognized by users, resulting in increased orders.

In this paper, the structural characteristics of this composite slab bridge shown in a static bending rupture test and a high-cycle fatigue test are described. Design principles such as methods for calculating cross section and ultimate strength are also proposed, and a highway bridge design method based on these principles is given. In addition, examples of fabrication and erection of new bridges are reviewed.

2 Features of Composite Slab Bridge

This bridge has the following features:

(1) It is possible to make the bridge depth significantly smaller than those of conventional bridges. When the span/depth ratio of this bridge is compared with those of conventional bridges, it is found, as shown in **Fig. 2**, that, bridge depth can be reduced as low as a span/depth ratio of 33 or above, compared with 26 to 30 with steel deck plate girders and 18 to 22 with prestressed concrete girders.

(2) Shear connectors such as studs become unnecessary, thereby permitting the use of a thinner concrete covering.

(3) Since the steel girder is covered with expansive concrete, the slab bridge has high flexural rigidity and develops only little deflection under live loads.

(4) Since the bottom plates can also be used as permanent forms. Forms and timbering work become unnecessary for placing of concrete.

(5) Field construction work is easy and safe, and a shortening of the construction placing is possible.

(6) Through the use of the atmospheric corrosion resisting steels, repainting becomes unnecessary, thereby lowering maintenance and repair costs.

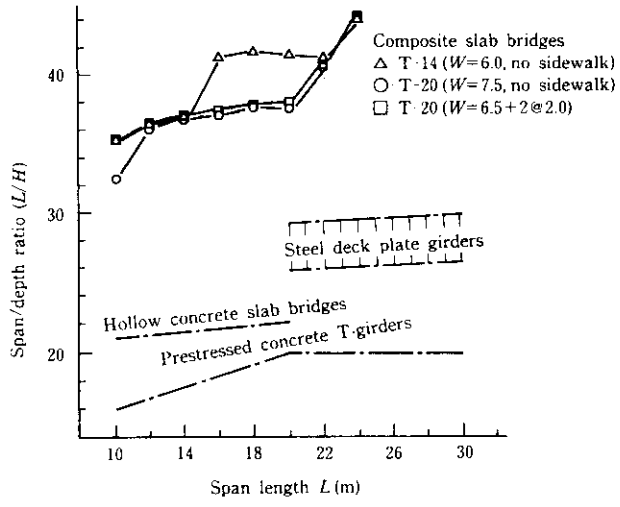

Fig. 2 The span/depth ratios for road bridges in Japan

3 Clarification of Structural Characteristics[2)]

3.1 Purpose of Experiments

A static bending rupture test was conducted on a composite slab specimen with the aim of verifying the characteristics in the elastic range and the integrity of the steel girder/slab concrete bond at the failure stage. Next, high-cycle fatigue and bending rupture tests were conducted on the other slab specimen with the aim of investigating the fatigue characteristics of composite slab under repeated loading.

3.2 Dimensions of specimens

The dimensions of the composite slab specimen used in the static test are shown in **Fig. 3**. T-shapes (248 × 199 × 9 × 14 mm) with protrusions were welded on the 12-mm thick bottom plate at a picth of 40 cm in the longitudinal direction, and D13 bars were arranged in the middle of the upper flange. The slab depth was 31 cm. In the specimen for the fatigue test, however, the slab depth was 21 cm and the bottom plate thickness was 8 mm, as shown in **Fig. 4**, in order to achieve economical cost performance. In both specimens, the maximum size of the coarse aggregate was 25 mm, and the water/cement ratio was 47%. Two kinds of ready mixed concrete having design strengths of 29.4 and 34.3 MPa were used for static and fatigue test specimens, respectively. An expansive admixture in a quantity of 30 kg/m^3 was used to prevent cracking of concrete due to dry shrinkage.

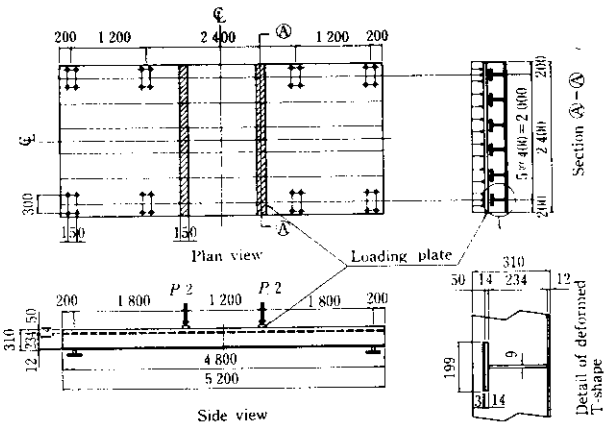

Fig. 3 Dimensions of composite slab specimen for bending rupture test

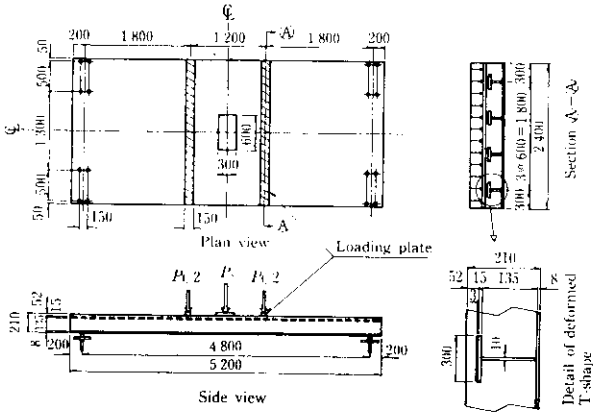

Fig. 4 Dimensions of composite slab specimen for high-cycle fatigue test

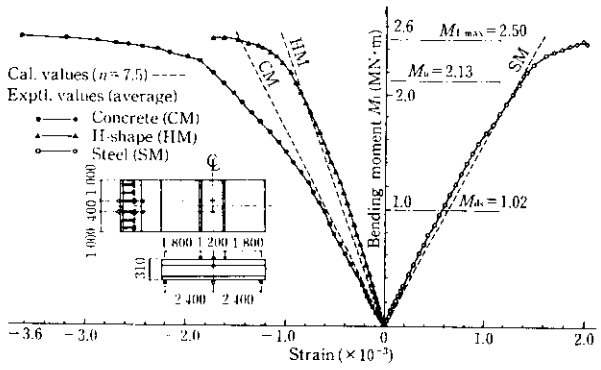

Fig. 6 Moment-strain curves at midspan section of composite slab in static test

3.3 Test Results and Discussion

3.3.1 Static bending repture test

Figure 5 shows the lateral distribution of bending stress at mid-span section when a concentrated load of 235 kN was applied to the center of the slab bridge. The experimental value was taken from the right-angle strain gauge, and the calculated value obtained by the converted sectional area method, in which the bending moment is obtained on the basis of isotropical slab theory. The experimental value is nearly equal to the calculated value, with load evenly distributed over the entire width. Thus, the validity of the calculation method for working stress using isotropical slab theory and the converted sectional area method was verified.

Figure 6 shows the relation between bending moment and strain at the cross section of the mid-span when 2-point concentrated line loads were applied. From this figure, it has been verified that (1) the experimental values are approximately equal to the calculated ones up to the bending moment (M_{ds}) stage, where the calculated stress of the bottom plate corresponds to the allowable tensile stress, (2) the ultimate bending compressive strain of concrete is 3.6×10^{-3}, which is larger than that of conventional reinforced concrete, (3) the ultimate bending moment is 2.50 MN · m which is about 1.2 times the calculated ultimate moment of 2.13 MN · m, obtained using stress distribution according to AASHTO, and (4) the steel girder and slab concrete remain in the unit superstructure at the failure stage.

3.3.2 High cycle fatigue test

Figure 7 shows the relation between the stress of the bottom plate and the number of cycles of repetition of concentrated loading applied to the center of the slab bridge. Up to the load of 157 kN in the initial loading, the experimental value was nearly equal to the calculated one obtained from the factors including the tensile stress of concrete. Thereafter, however, the experimental value became asymptotically to the calculated value in which the tensile stress of the concrete was neglected. In a repeated load range from 19.6 to 294 kN, residual stress after the initial loading slightly increased, but no increase in the amplitude of stress range was observed, and the residual stress remained at a nearly constant level during the 3.6 million cycle test.

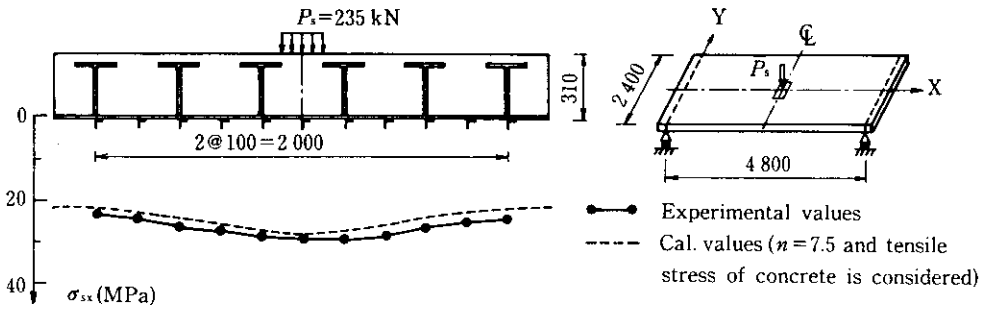

Fig. 5 Lateral distribution tensile stress at the midspan section in static test

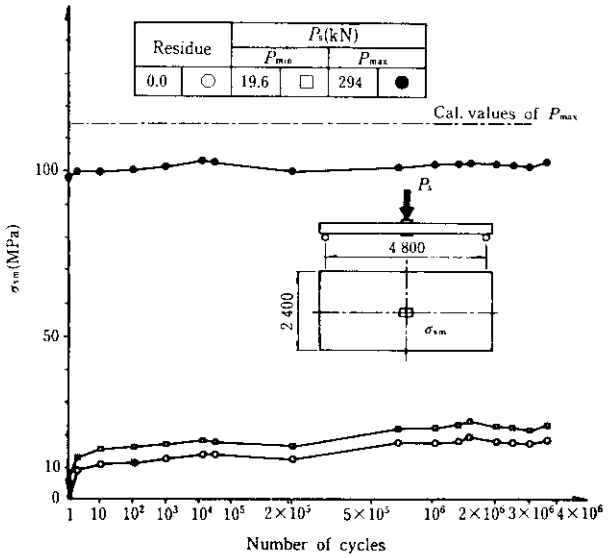

Fig. 7 Relation between number of cycles and tensile stress of steel at midspan section

4 Design Method[3)]

4.1 Design Calculation Method

4.1.1 Calculation of stress at section

When concrete is sufficiently bonded to steel girder and both the materials maintain a unit superstructure at the ultimate stage, it is possible, in general, to obtain the stress of the composite materials, neglecting the tensile stress of the concrete, on the basis of a converted sectional area method in which concrete in the compressed portion is converted into a cross section equivalent to steel by using n, ratio of moduli of elasticity between steel and concrete.

The distance y_{cu}, as shown in **Fig. 8**, from the upper extreme edge of the concrete to the neutral axis is obtained by Eqs. (1) and (2).

$$\frac{By_{cu}^2}{2n} + A_s(y_{cu} - g_s) = 0 \cdots\cdots\cdots\cdots\cdots (1)$$

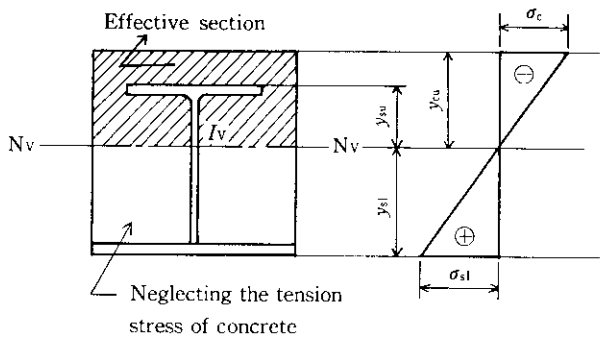

Fig. 8 Symbols in working stress design

$$y_{cu} = \frac{nA_s}{B}\left(-1 + \sqrt{1 + \frac{2Bg_s}{nA_s}}\right) \cdots\cdots\cdots (2)$$

where

B: Intervals of deformed flange T-shapes (cm)
A_s: Sectional area of steel girder (cm^2)
g_s: Distance from extreme upper edge of concrete to center of gravity
n: Elastic modulus ratio of steel to concrete

Next, the moment of inertia I_V concerning the neutral axis of the composite slab converted into steel is obtained by Eq. (3).

$$I_V = \frac{By_{cu}^3}{3n} + I_s + A_s(g_s - y_{cu})^2 \cdots\cdots\cdots (3)$$

where

I_s: Moment of inertia of steel-girder cross section (cm^4)

Therefore, the stress of the composite slab which receives bending moment M_V is calculated by Eqs. (4) and (5).

$$\sigma_c = -\frac{M_V}{nI_V} \times y_{cu} \cdots\cdots\cdots\cdots\cdots (4)$$

$$\sigma_{sl} = \frac{M_V}{I_V} \times y_{sl} \cdots\cdots\cdots\cdots\cdots (5)$$

where

σ_c: Extreme fibre stress at upper edge of concrete (MPa)
σ_{sl}: Stress of bottom steel plate (MPa)
y_{sl}: Distance from neutral axis of composite cross section to bottom steel plate (cm)

4.1.2 Calculation of horizontal shearing stress

When it is assumed that protrusions on the upper flange transmit horizontal shearing force, shearing strees τ_d generated at the protrusions can be calculated by Eq. (6).

$$\tau_d = \frac{Q_c}{I_V b_f} \times S_d \cdots\cdots\cdots\cdots\cdots (6)$$

where

Q_c: Statical moment of area converted into steel on compressive side of concrete (cm^3)
b_f: Upper flange width (cm)
S_d: Shearing force (N)

4.2 Calculation of Ultimate Strength

The stress condition at the failure stage is assumed to be as follows:

(1) Stress distributions of steel and concrete are assumed to be rectangular, as shown in **Fig. 9**.
(2) Tensile stress of concrete is neglected.

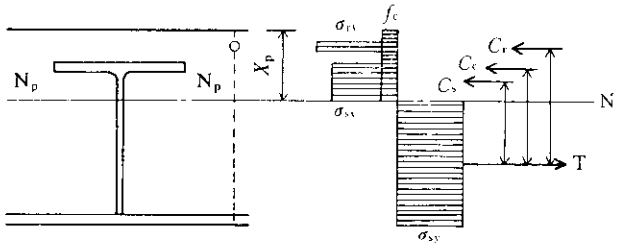

Fig. 9 Stress diagrams in ultimate strength for composite slab bridge

(3) Sectional area of steel is not subtracted from that of concrete.
(4) Ultimate strengths of concrete f_c, reinforcing bar σ_{ry}, and steel σ_{sy} are defined as 85% of design strength of concrete and nominal yield point of steels, respectively.

Distance X_p from the upper extreme of concrete to the neutral axis at failure stage can be obtained by Eq. (7).

$$\sum A_i \sigma_i = 0 \quad \cdots\cdots (7)$$

When X_p is obtained, M_u can be obtained as the ultimate resistant moment around the neutral axis by Eq. (8).

$$M_u = \sum A_i \sigma_i x_{pi} \quad \cdots\cdots (8)$$

where

x_{pi}: Distance from the neutral axis to the center of gravity position of sectional area A_i of each member.

Maximum resistant moment M_{uc} with respect to applied load is a corrected value obtained by subtracting moment M_d due to dead weight from M_u. When the distance from the fulcrum position to the loading point is denoted by L_p, maximum load P_{uc} can be obtained from Eq. (9).

$$P_{uc} = \frac{2M_{uc}}{L_p} \quad \cdots\cdots (9)$$

Maximum shearing stress τ_{bu} necessary for flange protrusions is theoretically given by Eq. (6). Provided that, in Eq. (6), the quantity that corresponds to Q_c is the compressive force of concrete, the quantity that corresponds to I_V is $\Sigma A_i \sigma_i x_{pi}$, namely M_u, τ_{bu} is expressed by Eq. (10).

$$\tau_{bu} = \frac{BX_p f_c}{M_u b_f} \times S_u \quad \cdots\cdots (10)$$

τ_{bu} in case of slab bridge with a centrally-symmetrical 2-point load is given by the following equation:

$$\tau_{bu} = \frac{BX_p f_c}{M_u b_f} \times \frac{P_u}{2} = \frac{BX_p f_c}{L_p b_f} \quad \cdots\cdots (11)$$

4.3 Design Procedure

Design is carried out as shown below based on "Specifications for Highway Bridge"[4] (hereinafter called the Spec.).

(1) Load
The calculation of sectional force due to live load must conform to the Spec. III.6.4.[4] Specifically, in the span direction, at mid-span design bending moment due to live load is calculated by assuming that in the case of a simply supported slab bridge whose span length exceeds 10 m, bending moment is uniformly shared by all main girders. (Bending moment is calculated by considering the slab bridge as a girder which receives a uniform load of 3.43 kPa over the full width of the sidewalk and principal L load over the full width of roadway.)

(2) Impact Coefficient
To calculate impact coefficient i, the following equations for a reinforced concrete bridge in Table 2.1.7 of the Sepc. I[4] are applied:

$$i = \frac{7}{20 + L} \quad \text{(for L load)}$$

$$i = \frac{20}{50 + L} \quad \text{(for T load)}$$

where

L: Span length (m)

(3) Main Materials
As a rule, atmospheric corrosion resisting steel plates (SMA41W or 50W) are used for bottom plates, and SM41 or SM50Y are used for deformed flange T-shapes. For slab concrete, design strength must be 26.5 MPa or above, and expansive concrete with a unit admixture quantity of 30 kg/m^3 must be used.

(4) Determination of Main Girder Cross Section
Sectional stress is calculated according to the Spec. II.9[4]; assuming that the dead loads of the steel girder and slab concrete are supported only by the steel girder, and dead load after placing of concrete and live load are supported by the complete composite section, sectional stress is calculated using Eqs. (4) and (5).

(5) Horizontal Shearing Stress
Horizontal shearing stress generated at the protrusions on the upper flange is calculated using Eq. (6). Allowable shearing stress at the protrusions is assumed to be 17 kgf/cm^2 or above, which is the same as that of a deformed bar.

(6) Allowable Value of Live Load Deflection
The maximum deflection δ due to live load must be $L/600$ or below.

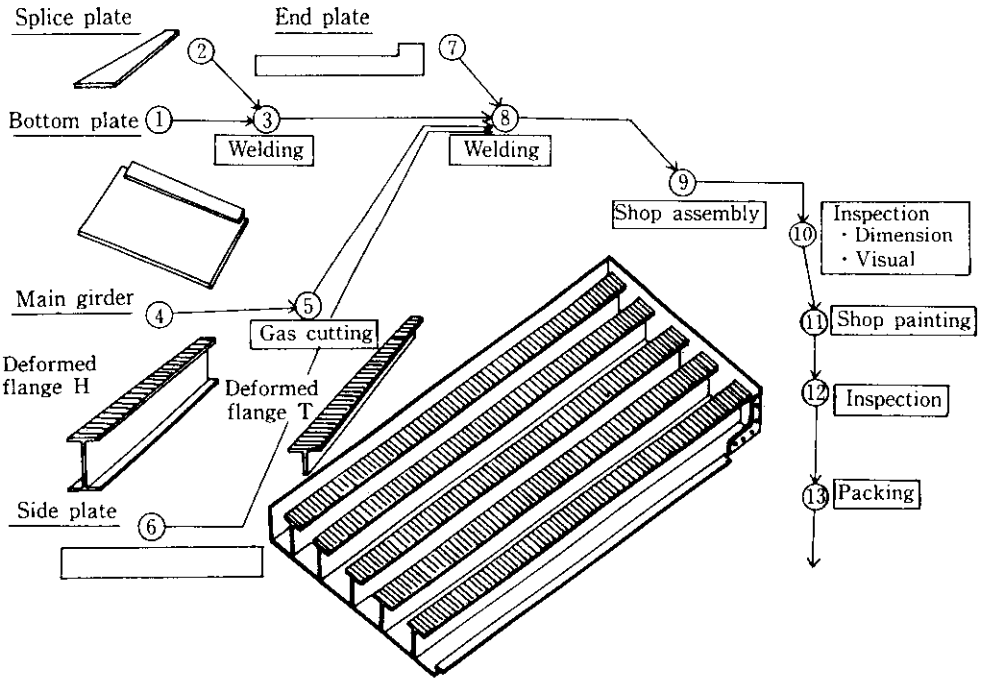

Fig. 10 Shop assembly process

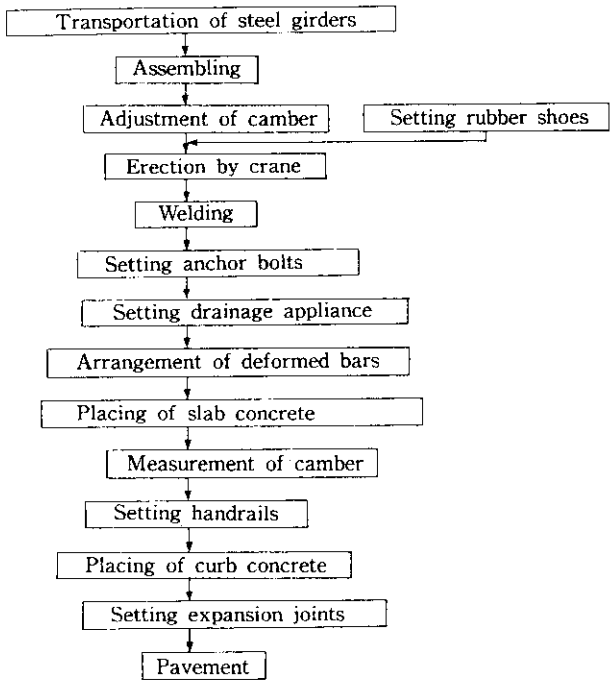

Fig. 11 Erection process

5 Construction Procedure and Application

5.1 Construction Procedure

Shop assembly and field erection are carried out according to the procedure shown in **Fig. 10**. Since deformed flange T-shapes are made by gas-cutting deformed H-shapes into halves, straightening and cambering become necessary. After T-shapes are welded to a bottom plate, side and end plates are fitted. In forming the field butt-welded joints of the upper flanges, a welding test is sometimes conducted beforehand to determine welding conditions. Next, various members are provisionally assembled on a sturdy support pedestal under no-stress conditions to check for fabrication accuracy.

The operation sequence of field erection is shown in **Fig. 11**. The important work in field erection is the field welding of joints and placing of slab concrete. Field butt-welded joints of the upper flange in the direction perpendicular to the span are checked by the X-ray radiographic test for any internal defects. The web and the bottom plate are connected by high-tension bolts. **Photo 1** shows the steel girder erection for the top slab of the Mukaihara Tunnel; **Photo 2** shows the field butt-welding operation for the upper flange of deformed flange T-shapes for the Kawatoku Bridge.

For the slab concrete, expansive concrete is used to prevent the concrete from developing cracks due to drying shrinkage. Careful quality control is maintained with the expansive concrete so as to achieve design strength. Since the placing of concrete greatly affects camber, care is necessary. In general, placing of concrete begins near the mid-span of the bridge and continues from the center towards both ends. In particular, careful

Photo 1 Steel girder erection for the top slab of the Mukaihara Tunnel

Photo 2 Field butt-welding of upper flange of deformed flange T-shapes for the Kawatoku Bridge

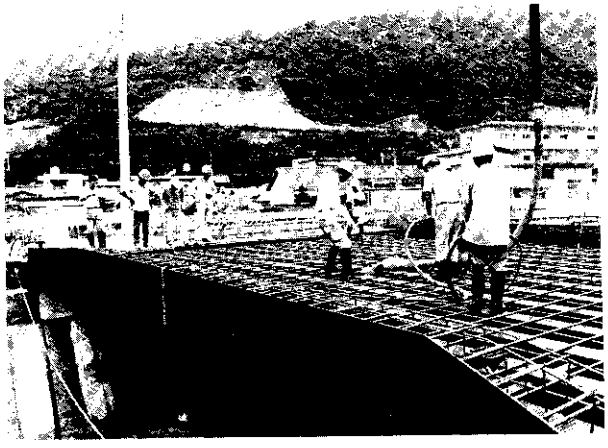

Photo 3 Placing of slab concrete for the Minato Bridge

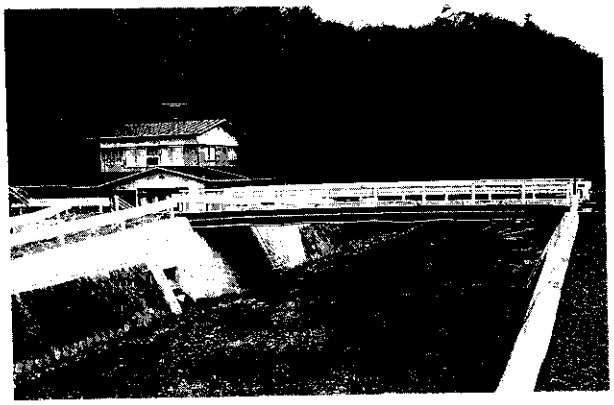

Photo 4 Matsudate Bridge

attention is required with skew bridges, because torsion may develop depending on the placing sequence of concrete. In principle, concrete placing must be continuous and no joints are permissible. To obtain perfect bonding between concrete and deformed flange T-shapes, compaction must carried out carefully using a rod vibrator, and curing of the concrete must be carried out as soon as possible after placing. **Photo 3** shows the placing of concrete for the Minato Bridge.

5.2 Examples of Construction

Since the commencement of sales of this type of bridge in 1982, many enquiries have been received. Twenty-one such bridges have been constructed, and four bridges are scheduled to be completed in fiscal 1985; construction of four additional bridges has also been provisionally decided. Examples of these bridges are shown in **Table 1**, and **Photo 4** shows a view of the completed Matsudate Bridge. This type of bridge is frequently adopted where it is necessary to keep girder height as low as possible due to the height of the access road, where securing of depth is absolutely required, or where the bridge has a skew angle as sharp as 45°.

6 Conclusions

Through a bending rupture test and a high-cycle fatigue test, it has been confirmed that the sectional stress of the composite slab bridge can be obtained by the so-called "converted sectional area method," in which sectional force calculated according to the Spec.III.6 (Slab Bridges) is borne by a composite cross section of steel and compressive concrete formed into a unit superstructure. It has also been confirmed that even at the failure stage, the steel girder and slab concrete remain integrated as a unit superstructure, and that this bridge can satisfactorily withstand repetitive

Table 1 Summary of composite slab bridge specifications

Bridge Name	Location	Loads*	Bridge length (m)	Width (m)	Skew angle	Slab depth (cm)	Span/depth ratio	Erection year	Remark
Top Slab of Tunnel (トンネル頂版)	Tokyo	T, L-14	17.500 (2@8.750)	19.900	90°	35.0	25	1983	See Photo 1
Matsudate Bridge (松館橋)	Iwate	T, L-14	16.700	5.200	70°	38.5	42	1984	Snow loads See Photo 4
Pedestrian Bridge (歩道橋)	Hokkaido	350 kg/m²	18.000	1.800	90°	33.3	53	1984	Snow loads
Sengen-Uemachi Bridge (浅間上町橋)	Shizuoka	T, L-6	10.700	3.200	79°	33.4	32	1984	
Showa Bridge (昭和橋)	Tokyo	T, L-14	9.200	4.100 ~5.700	90°	24.9	34	1985	
Osawagawa Bridge (大沢川橋)	Nagano	T, L-20	10.500	7.700	45°	32.8	29	1985	
Minato Bridge (湊橋)	Ehime	T, L-20	11.600	8.200	90°	32.2	34	1985	See Photo 3
Kawatoku Bridge (川徳橋)	Aichi	T, L-14	49.600 (2@24.800)	6.200	90°	54.5	44	1985	See Photo 2
Shin-ebigawa Bridge (新海老川橋)	Chiba	T, L-14	13.800	6.700	85°	33.0	40	1985	
Higashichuo Bridge (東中央橋)	Tokyo	T, L-20	22.651	9.200	42°	54.5	40	1985	
Nangu Bridge (南宮橋)	Tokyo	T, L-20	20.870	9.200	50°	53.1	38	1986	

*Note: Specifications for highway bridges part I common (Japan Road Association)

loading of 3.6 million cycles, corresponding to three times the T load stipulated by the Spec. In view of the above findings, the authors have established a design calculation method which observes stipulations of the Spec. and reflects the outcome of the present tests, and accordingly have prepared a design procedure.

The span/depth ratios of this bridge are as high as over 33 and slab's depth is significantly smaller than those of conventional bridges. Therefore, the number of orders for this bridge is yearly increasing as new construction bridges for river improvement and railway overbridges.

In the future, the authors will prepare guidelines for fabrication and erection to make it possible to apply this bridge to any kind of road alignment and, further, plan research on a hollow type composite slab and a continuous composite slab bridge, aimed at expanding applicable span length.

References

1) M. Sato, M. Hara, M. Ishiwata, and E. Yamanaka: "Introducing Composite Structures Using Newly Developed Checkered Steel Pipe and Deformed Flange H-shapes" *Kawasaki Steel Technical Report*, No. 5 (1982), 94-104
2) T. Yamasaki, T. Kaneko and M. Sato: "Composite Slab Bridges Using Deformed Flange T-shapes," 12th Congress of International Association for Bridge and Structural Engineering, Vancouver, (1984), 385-392
3) S. Tanaka, M. Sato, K. Hamada and T. Kasuga: "Structural Characteristics of Composite Bridges Using Deformed Flange T-shapes," the First East Asian Conference on Structural Engineering and Construction, Bangkok, (1986), 1417-1428
4) Japan Road Association: Specification for Highway Bridges; Part I, Common; Part II, Steel Bridges; Part III, Concrete Bridges